Journal of Power Sources 196 (2011) 9356–9360

Contents lists available at ScienceDirect

Journal of Power Sources

journal homepage: www.elsevier.com/locate/jpowsour

Short communication

Ultrasonic synthesis of nitrogen-doped carbon nanofibers as platinum catalyst support for oxygen reduction

Yue Jiang[a], Jia Zhang[a], Yuan-Hang Qin[a], Dong-Fang Niu[a], Xin-Sheng Zhang[a,*], Li Niu[b], Xing-Gui Zhou[a], Tian-Hong Lu[b,c], Wei-Kang Yuan[a]

[a] State Key Laboratory of Chemical Engineering, East China University of Science and Technology, Shanghai 200237, China
[b] State Key Laboratory of Electroanalytical Chemistry, Chang Chun Institute of Applied Chemistry, Chinese Academy of Sciences, Changchun 130022, China
[c] Department of Chemistry, Nanjing Normal University, Nanjing 210097, China

ARTICLE INFO

Article history:
Received 8 June 2011
Received in revised form 7 July 2011
Accepted 8 July 2011
Available online 19 July 2011

Keywords:
Carbon nanofiber
Nitrogen-doping
Oxygen reduction reaction
Electrocatalysis

ABSTRACT

Oxygen- and nitrogen-containing groups are successfully introduced onto the carbon nanofiber (CNF) surfaces by sonochemical treatment in mixed acids (concentrated sulfuric acid and nitric acid) and ammonia, respectively. Pt electrocatalysts supported on the acid-treated CNF (CNF-O) and ammonia-treated CNF (CNF-ON) are prepared and the effect of CNF surface functional groups on the electrocatalytic activities of supported catalysts for oxygen reduction reaction (ORR) is investigated. High resolution transmission electron microscopy reveals that Pt particles are uniformly dispersed on the two CNF supports and the CNF-ON supported Pt nanoparticles have a smaller average particle size and a more uniform particle size distribution. Cyclic voltammetric analysis shows the Pt/CNF-ON has a larger electrochemically active surface area than Pt/CNF-O. Rotating disk electrode measurements show that the Pt/CNF-ON exhibits a considerably higher electrocatalytic activity toward ORR as compared with Pt/CNF-O. It is believed that the good electrocatalytic activity of Pt/CNF-ON can be attributed to the smaller Pt particle size and more uniform particle size distribution, to the synergistic effect and the enhanced Pt–CNF-ON interaction, and to the unique structural and electronic properties of CNF-ON.

1. Introduction

In spite of tremendous efforts to develop highly efficient oxygen reduction reaction (ORR) electrocatalyst for fuel cell applications, Pt remains the catalyst of choice at least for ORR in acidic media [1,2]. However, the high cost and low abundance of Pt greatly limit the practical application of fuel cells. To enhance the utilization of Pt catalyst so as to reduce the Pt required, several strategies have been explored, one of which is to employ nano-carbon materials as a support for higher dispersion of Pt catalysts [3]. Carbon nanofibers (CNFs), as a new catalyst support material, have attracted considerable attention in recent years because of their special electrical and structural properties [4,5].

However, the uniform dispersion of Pt nanoparticles on CNFs remains a formidable challenge because of the inert and hydrophobic nature of the CNF surface [6,7]. The introduction of functional groups onto CNF surface, which are expected to help improve the hydrophilic properties of CNF and stabilize metal particles on the CNF surface [8,9], is an attractive approach to overcome the above challenge. Oxygen-containing groups, which can be introduced onto CNF surface by oxidizing CNF with aqueous solutions of acids or oxidizing agents, are the most widely introduced functional groups [10,11].

Recently, the nitrogen-doped carbon nanotubes (CNTs) as catalyst support have drawn increasing attention. Saha et al. [12] prepared Pt nanoparticles supported on CNTs and CNx (nitrogen-doped CNTs) and found highly dispersed Pt nanoparticles with smaller size (2–3 nm) and higher electrochemical Pt surface area as well as higher fuel cell performance were obtained for CNx.

Nitrogen doping of CNTs can be divided into two categories: doping directly during the synthesis of CNTs and the post-treatment of pre-synthesized CNTs with nitrogen-containing precursor (N_2, NH_3, HCN, etc.) [13]. The direct doping methods such as arc-discharge [14,15], chemical vapor deposition (CVD) [16,17] are similar to those used to synthesize pure CNTs. Most of the post-dopings are carried out in nitrogen-containing atmosphere at high temperatures.

In this work, we developed a simple post-doping method to synthesize nitrogen-doped CNFs using a sonochemical process and the electrocatalytic activity of the Pt nanoparticles supported on the nitrogen-doped CNFs for ORR was evaluated.

* Corresponding author. Tel.: +86 21 64253469; fax: +86 21 64253528.
E-mail address: xszhang@ecust.edu.cn (X.-S. Zhang).

0378-7753/$ – see front matter © 2011 Elsevier B.V. All rights reserved.
doi:10.1016/j.jpowsour.2011.07.036

2. Experimental

2.1. Functionalization of CNFs

The fishbone CNFs (f-CNFs) purchased from Shenzhen Nanotech Port Co. Ltd. were sonochemically treated in mixed acids (concentrated sulfuric acid and nitric acid) to introduce oxygen-containing groups onto CNF surface [18]. Briefly, 1.00 g of the as-purchased CNFs was sonochemically treated in a solution containing 188 ml con. HNO_3, 160 ml con. H_2SO_4 and 12 ml de-ionized H_2O for 2 h in a laboratory ultrasonic bath (Shanghai Shenyuan Ultrasound Machines Ltd., 300 W and 40 kHz) at 60 °C. After surface treatment, the CNFs were filtered and washed thoroughly with de-ionized water before being dried at 120 °C for 12 h. The acid-treated CNF was labeled as CNF-O. Two hundred milligrams of CNF-O were sonochemically treated in 100 ml of ammonia for 3 h in the same ultrasonic bath at 60 °C to introduce nitrogen-containing groups onto CNF-O. Filtration, washing and drying procedures were the same as for the CNFs treated in mixed acids as described above. The ammonia-treated CNF-O was labeled as CNF-ON.

2.2. Preparation of Pt/CNF catalyst

The preparation of Pt/CNF electrocatalysts with a Pt content of 26.7 wt% was carried out in ethylene glycol (EG) solutions of H_2PtCl_6 precursor salts, and the procedure was described as follows. First, 50 mg of the surface-treated CNF (CNF-O or CNF-ON), 13.80 ml aqueous solution of 0.00680 M H_2PtCl_6 and 2 ml of 0.1 M KOH were added into 25 ml of ethylene glycol and stirred with ultrasonic treatment for 20 min at room temperature. Then the solution was heated in a three-neck round bottom flask connected with a condenser at 70 °C for 5 h with constant stirring. The resultant solid was filtered and washed thoroughly with de-ionized water and then dried at 120 °C for 12 h. The CNF-O and CNF-ON supported Pt nanoparticles were labeled as Pt/CNF-O and Pt/CNF-ON, respectively.

2.3. Preparation of Pt/CNF modified glassy carbon (Pt/CNF/GC) electrode

The Pt/CNF catalyst was dispersed in a 0.5 wt.% Nafion solution by ultrasonication to obtain a homogenous suspension with a concentration of 10 mg ml^{-1}. The Pt/CNF/GC electrode was obtained by pipetting 3 μl aliquot of the suspension onto a GC electrode (5 mm in diameter) surface and allowing the solvent to evaporate in air. Before surface modification, the GC electrode was polished to a mirror finish with 30 nm alumina slurry, washed successively with acetone, ethanol and water, and then subjected to ultrasonic agitation for 5 min in ultrapure water and dried in air for 30 min. The obtained Pt/CNF/GC electrode was dried at room temperature and then placed in ambient air for use. The Pt/CNF-O and Pt/CNF-ON modified GC electrodes were labeled as Pt/CNF-O/GC and Pt/CNF-ON/GC, respectively.

2.4. Catalyst characterization

The surface area measurements of CNF supports were performed on an ASAP 2010N surface area and porosity analyzer (Micromeritics, USA). Surface areas were obtained using the Brunauer–Emmett–Teller (BET) method. The X-ray photoelectron spectroscopy (XPS) carried out using a Kratos AXIS Ultra DLD spectrometer with monochromatic Al Kα radiation at a power of 45 W was used to characterize the composition of CNF supports. The morphologies of the Pt/CNF catalysts were characterized by high resolution transmission electron microscope (HRTEM, FEI Tecnai G^2 S-Twin) operated at 200 kV. The X-ray diffraction (XRD) patterns of the Pt/CNF catalysts were analyzed by an X-ray diffractometer (D/MAX 2550 VB/PC, RIGAKU) using a Cu Kα source operated at 40 kV at a scan rate of 2° min^{-1}. Electrochemical measurements were carried out on a PGSTAT 30 electrochemical workstation (Eco Chemie B.V., the Netherlands) in a 0.5 M H_2SO_4 solution at room temperature. A conventional three-electrode cell consisting of the prepared Pt/CNF/GC as the working electrode, a Pt wire as the counter electrode and a Ag/AgCl (10 wt.% KCl) electrode as the reference electrode was used for electrochemical characterizations. The rotating disk electrode measurements were also carried out using the autolab PGSTAT 30 workstation. The working electrode was fabricated by loading 3 μl aliquot of the suspension onto a 5 mm GC disk of the RDE (Pine Instrument Co.).

Table 1
BET surface areas and surface compositions of CNF-P, CNF-O and CNF-ON supports.

Sample	BET surface area ($m^2\ g^{-1}$)	Element content (atomic fraction, %)		
		C	O	N
CNF-P	102.03	98.55	1.45	0
CNF-O	119.99	91.08	8.92	0
CNF-ON	120.59	93.39	5.59	1.02

3. Results and discussion

3.1. Surface area measurements and XPS analysis

Table 1 shows the BET surface areas and surface compositions of CNF-P (untreated CNF), CNF-O and CNF-ON supports. It can be found that the surface area of CNFs was increased from 102.03 $m^2\ g^{-1}$ to 119.99 $m^2\ g^{-1}$ after sonochemical treatment in mixed acids, which may result from a partial opening of the CNFs. The sonochemical treatment of CNF-O in ammonia caused only a negligible increase in surface area, indicating that the structure of CNF-O did not change much after its sonochemical treatment in ammonia.

As shown in Table 1, the oxygen content was greatly increased after the CNF-P was sonochemically treated in mixed acids, while the nitrogen element was not detectable even on CNF-O, indicating that it is not easy to nitrate CNFs by oxidation treatment of CNFs even in nitrogen-containing acid (nitric acid). Nitrogen element was successfully incorporated onto CNF-O after its sonochemical treatment in ammonia. The incorporation of nitrogen may proceed by the partial substitution of oxygen atoms by nitrogen atoms during the ammonia treatment process, as evidenced by the decreased oxygen content of CNF-ON as compared with CNF-O.

The successful incorporation of nitrogen onto CNFs suggests that the sonochemical treatment is a promising process for the preparation of nitrogen-doped carbon materials due to its distinct advantages, such as mild reaction conditions, convenient operation and time saving, as compared with the traditional processes which often need long reaction time and high reaction temperature.

3.2. HRTEM characterizations of Pt/CNFs

Fig. 1(a) and (c) presents the HRTEM images of the Pt/CNF-O and Pt/CNF-ON catalysts, respectively. Both CNF-O and CNF-ON were decorated with highly dispersed Pt nanoparticles, indicating that sonochemical treatment is an effective method to uniformly import functional groups onto CNFs. As shown in Fig. 1(b) and (d), the average particle size of Pt/CNF-O is larger than that of Pt/CNF-ON, i.e., 2.23 nm for Pt/CNF-O and 1.82 nm for Pt/CNF-ON, and the particle size distribution of Pt/CNF-O is broader than that of Pt/CNF-ON. It is believed that the smaller particle size and narrower particle size distribution exhibited by Pt/CNF-ON can be attributed to the greater number of defective sites the nitrogen-containing functional

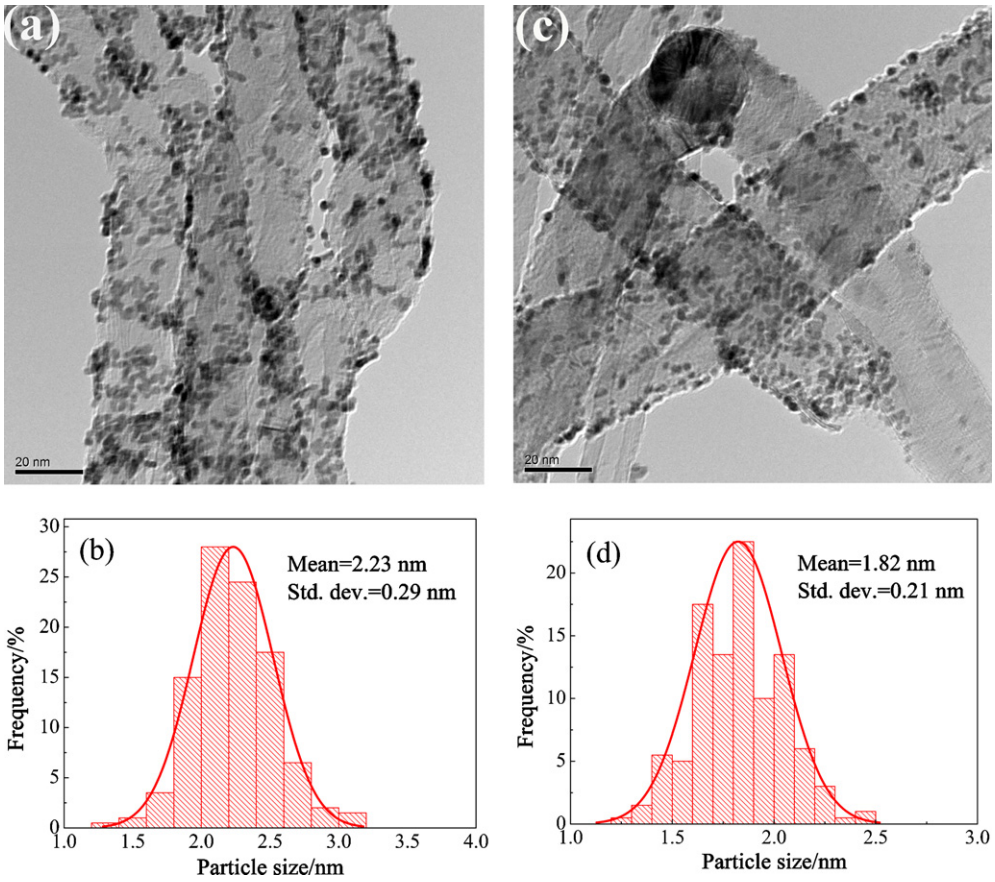

Fig. 1. HRTEM images of Pt/CNF-O (a) and Pt/CNF-ON (c) along with the corresponding particle size histograms based on the measurement of over 200 Pt nanoparticles on Pt/CNF-O (b) and Pt/CNF-ON (d).

groups yielded [19]. The incorporation of nitrogen atoms onto CNFs favours the formation of pentagons and heptagons [20] and results in more disorder in the graphene stacking due to the propensity of incorporated nitrogen [21]. The great number of defective sites on the CNF-ON support can provide more initial nucleation sites for the deposition of Pt [20,22], which thus lead to a smaller average particle size and a narrower particle size distribution.

3.3. XRD measurements

Fig. 2 shows the XRD patterns of the Pt/CNF-O (a) and Pt/CNF-ON (b) catalysts.

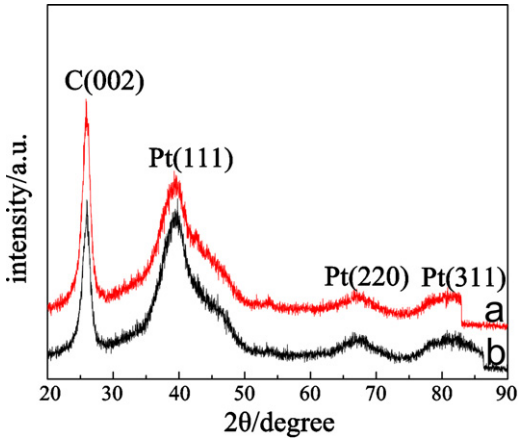

Fig. 2. XRD patterns of Pt/CNF-O (a) and Pt/CNF-ON (b) catalysts.

The diffraction peaks at 2θ values of 39.9°, 67.5° and 81.2° on the XRD patterns of Pt/CNFs catalysts can be assigned to the (1 1 1), (2 2 0) and (3 1 1) lattice planes of the face-centered cubic (fcc) Pt crystal structure. The average particle sizes of Pt in the case of Pt/CNF-ON and Pt/CNF-O calculated from the Pt (1 1 1) peak using Scherrer's equation [23] were both 1.8 nm.

3.4. Electrochemical surface area

Fig. 3 shows the cyclic voltammetry (CV) curves of the two electrodes recorded at room temperature in a N_2 saturated 0.5 M H_2SO_4 solution at a sweep rate of 50 mV s^{-1}. The electrochemi-

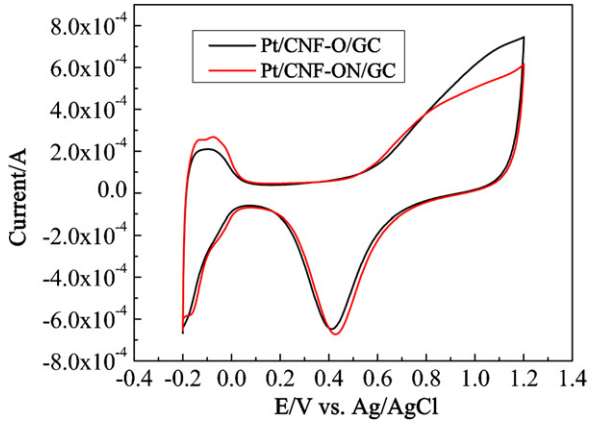

Fig. 3. Cyclic voltammograms in a N_2 saturated 0.5 M H_2SO_4 solution for Pt/CNF-O/GC and Pt/CNF-ON/GC.

cally active surface area (ECSA) was calculated by measuring the charge collected in the hydrogen adsorption/desorption region after double-layer correction and assuming a value of 0.21 mC cm^{-2} for the electroactive Pt surface [24]. The charge under the hydrogen adsorption/desorption region for Pt/CNF-ON/GC electrode was 1.03×10^{-2} C cm^{-2}, whereas that for the Pt/CNF-O/GC electrode was 9.328×10^{-3} C cm^{-2}. The increase in ECSA for Pt/CNF-ON/GC may be mainly ascribed to the smaller Pt particle size of Pt/CNF-ON/GC.

3.5. Rotating disk electrode studies of oxygen reduction

ORR is a rather complex multistep process. In acidic solution, ORR involves a four-electron pathway (Eq. (1)), with oxygen reduction directly to water and a two-step (Eq. (2)), two-electron pathway with hydrogen peroxide as intermediate product. The main products of ORR are H_2O_2 and H_2O, depending on electrode materials, electrode potential, and solution composition [19,25].

$$O_2 + 4H^+ + 4e^- \rightarrow 2H_2O \quad (1)$$

$$O_2 + 2H^+ + 2e^- \rightarrow H_2O_2 \quad (2)$$

$$H_2O_2 + 2H^+ + 2e^- \rightarrow 2H_2O \quad (3)$$

$$2H_2O_2 \rightarrow 2H_2O + O_2 \quad (4)$$

To get better understanding of the ORR route, the linear sweep voltammetric measurements were performed for Pt/CNF-O/GC and Pt/CNF-ON/GC electrodes in an O_2 saturated 0.5 M H_2SO_4 solution at a scan rate of 10 mV s^{-1} at room temperature, as shown in Fig. 4. The RDE results obtained were similar for both electrodes, with the limiting current density increases with increasing rotation rate.

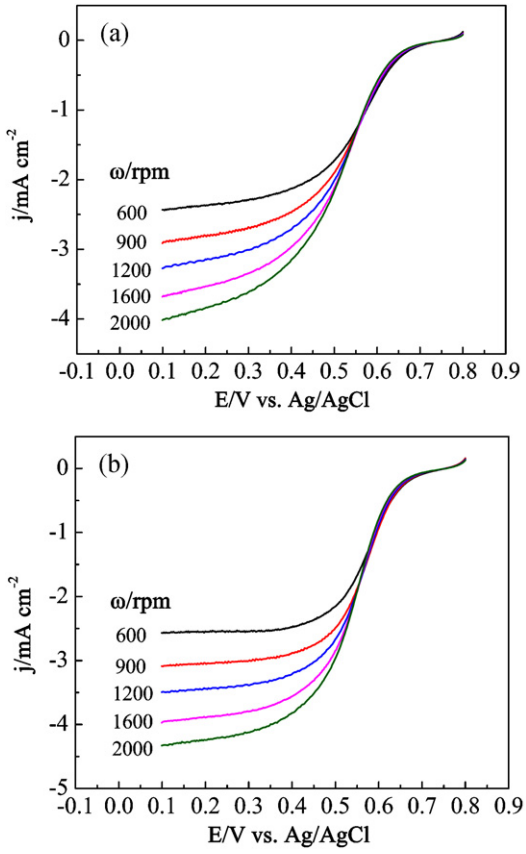

Fig. 4. RDE voltammetry curves for oxygen reduction on Pt/CNF-O/GC (a) and Pt/CNF-ON/GC (b) electrodes in an O_2 saturated 0.5 M H_2SO_4 with a scan rate of 10 mV s^{-1}.

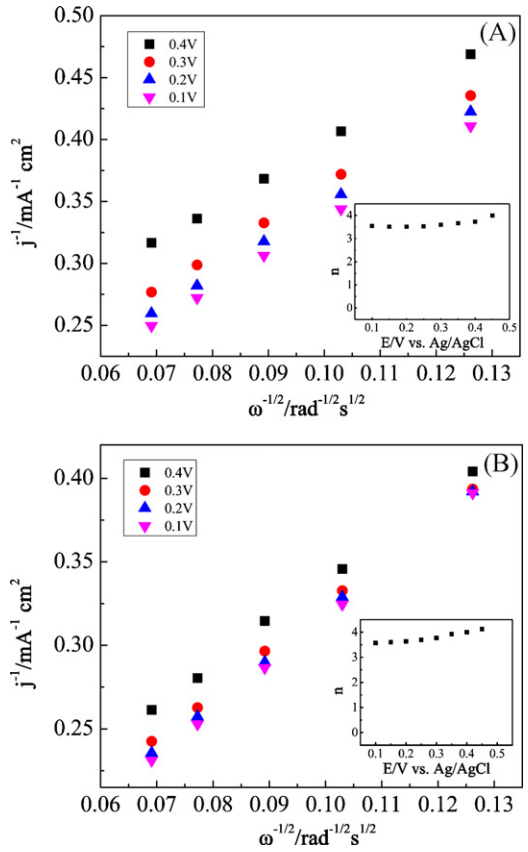

Fig. 5. Koutecky–Levich plots for oxygen reduction on Pt/CNF-O/GC (a) and Pt/CNF-ON/GC (b) electrodes; the inset shows the dependence of n on potential.

The number of electrons transferred per O_2 molecule (n) was calculated from the Koutecky–Levich (K–L) equation [26]

$$\frac{1}{j} = \frac{1}{j_k} + \frac{1}{j_d} = -\frac{1}{nFkC^b_{O_2}} - \frac{1}{0.6nFD^{2/3}_{O_2}\nu^{-1/6}c^b_{O_2}\omega^{1/2}} \quad (5)$$

where j is the measured current density, j_k and j_d are the kinetic and diffusion-limited current densities, respectively; k is the electrochemical rate constant for oxygen reduction, D_{O_2} is the diffusion coefficient of oxygen (1.8×10^{-5} cm^2 s^{-1}) [27], $C^b_{O_2}$ is the concentration of oxygen in the bulk (1.13×10^{-6} mol cm^{-3}) [27], and ν is the kinematic viscosity of the solution (0.01 cm^2 s^{-1}) [28].

The Koutecky–Levich plots of oxygen reduction on Pt/CNF-O/GC and Pt/CNF-ON/GC electrodes are shown in Fig. 5. The K–L lines are linear and parallel, indicating first-order ORR kinetics with respect to dissolved oxygen [29].

The inset of Fig. 5(a) and (b) compared the n values calculated from the K–L equation at various potentials. For both electrodes, the n value was close to four over the whole range of potentials studied, showing that the reduction of oxygen proceeds predominantly by the $4e^-$ pathway (Eq. (1)).

The current–potential curves recorded at room temperature for Pt/CNF-O/GC and Pt/CNF-ON/GC electrodes in an O_2 saturated 0.5 M H_2SO_4 at a scan rate of 10 mV s^{-1} in the cathodic direction at a rotation speed of 1600 rpm are shown in Fig. 6. It is evident that Pt/CNF-ON/GC electrode exhibited a better electrocatalytic activity than Pt/CNF-O/GC with respect to both half-wave potential and diffusion-limited current density. The half-wave potential of Pt/CNF-ON/GC was found to be approximately 40 mV more positive than that of Pt/CNF-O/GC.

The results we obtained reveal that the Pt/CNF-ON/GC electrode is more active than Pt/CNF-O/GC toward ORR in 0.5 M H_2SO_4

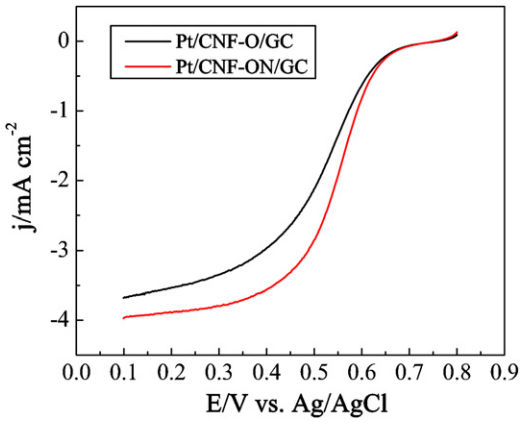

Fig. 6. Current–potential curves for Pt/CNF-O/GC and Pt/CNF-ON/GC electrodes in an O_2 saturated 0.5 M H_2SO_4 at a scan rate of 10 mV s^{-1} in the cathodic direction at a rotation speed of 1600 rpm.

solution. The improved ORR activity exhibited by the Pt/CNF-ON/GC electrode as compared to the Pt/CNF-O/GC electrode may be attributed to several factors. Firstly, the Pt nanoparticles supported on CNF-ON exhibited smaller particle size and more uniform size distribution than those supported on CNF-O. It is well known that the catalytic activity of metal particles is strongly dependent on the particle size and distribution. The uniform distribution of Pt nanoparticles and relatively small particle size lead to a larger ECSA for Pt/CNF-ON/GC. A larger ECSA generally means a better catalytic activity. Secondly, a synergistic effect and an enhanced Pt-support interaction may exist between CNF-ON and the supported Pt nanoparticles. It is reported that nitrogen-doped carbon support can serve to electrochemically reduce ORR byproducts and intermediates, mainly hydrogen peroxide [30–32]. Shao et al. [13] confirmed Pt-based catalysts with nitrogen-doped carbon as support exhibited enhanced catalytic activity toward oxygen reduction, which can be attributed to the high dispersion of Pt nanoparticles and the modified interaction between Pt nanoparticles and the support. Finally, the unique electronic and structural properties of CNF-ON may also contribute to the enhanced ORR activity of CNF-ON supported Pt nanoparticles. Doping CNFs with nitrogen would yield a large number of defective sites on the CNF surfaces, which is proven to be an efficient method to regulate the structural and electronic properties of CNFs [19,33,34]. Higgins et al. [35] utilized ED-CNTs (N-CNTs synthesized from a nitrogen-rich ethylenediamine (ED) precursor solution) as Pt nanoparticle supports and found Pt/ED-CNTs displayed significantly enhanced electrocatalytic activity toward ORR when compared with nitrogen free Pt/CNTs, with the increase in performance being attributed to the distinct structural and electronic enhancements resulting from heterogeneous nitrogen doping.

4. Conclusions

In this work, the oxygen- and nitrogen-containing functional groups were introduced onto the CNF surface by sonochemical treatment in mixed acids (concentrated sulfuric acid and nitric acid) and ammonia, respectively. The Pt/CNF-ON/GC electrode exhibited a better electrocatalytic activity toward ORR compared with Pt/CNF-O/GC electrode. It is believed that the enhanced catalytic activity exhibited by the Pt/CNF-ON/GC electrode can mainly be attributed to the smaller Pt particle size and more uniform particle size distribution. The synergistic effect, the enhanced Pt–CNF-ON interaction, and the unique structural and electronic properties of CNF-ON may also contribute to the enhanced catalytic activity. This study highlights the importance of introducing surface functional groups especially nitrogen-containing groups onto CNFs as electrocatalyst support materials. The uniform Pt nanoparticles on CNF-ON support have shown high catalytic activity toward ORR, indicating the sonochemical process is a promising method to introduce nitrogen-containing groups onto CNF surfaces.

Acknowledgements

The present study was supported by the Nature Science Foundation of China (21073061), the open foundation of the State Key Laboratory of Electroanalytical Chemistry (Changchun Institute of Applied Chemistry, Chinese Academy of Sciences) and the State Key Laboratory of Physical Chemistry of Solid Surfaces (Xiamen University).

References

[1] H. Tang, J. Chen, Z. Huang, D. Wang, Z. Ren, L. Nie, Y. Kuang, S. Yao, Carbon 42 (2004) 191–197.
[2] Z. Chen, M. Waje, W. Li, Y. Yan, Angew. Chem. Int. Ed. 119 (2007) 4138–4141.
[3] B. Ijuki, C. Banks, R. Compton, J. Iran. Chem. Soc. 2 (2005) 1–25.
[4] R.J. Taylor, A.A. Humffray, J. Electroanal. Chem. 64 (1975) 63–84.
[5] C.A. Bessel, K. Laubernds, N. Rodriguez, R. Baker, J. Phys. Chem. B 105 (2001) 1115–1118.
[6] M.S. Saha, A. Kundu, J. Power Sources 195 (2010) 6255–6261.
[7] P. Serp, M. Corrias, P. Kalck, Appl. Catal. A: Gen. 253 (2003) 337–358.
[8] R.A. Sidik, A.B. Anderson, N.P. Subramanian, S.P. Kumaraguru, B.N. Popov, J. Phys. Chem. B 110 (2006) 1787–1793.
[9] G.G. Wildgoose, C.E. Banks, H.C. Leventis, R.G. Compton, Microchim. Acta 152 (2006) 187–214.
[10] T.G. Ros, A.J. Dillen Van, J.W. Geus, D.C. Koningsberger, Chem. Eur. J. 8 (2002) 1151–1162.
[11] K. Vaik, U. Mäeorg, F. Maschion, G. Maia, D. Schiffrin, K. Tammeveski, Electrochim. Acta 50 (2005) 5126–5131.
[12] M.S. Saha, R. Li, X. Sun, S. Ye, Electrochem. Commun. 11 (2009) 438–441.
[13] Y. Shao, J. Sui, G. Yin, Y. Gao, Appl. Catal. B: Environ. 79 (2008) 89–99.
[14] M. Glerup, J. Steinmetz, D. Samaille, O. Stephan, S. Enouz, A. Loiseau, S. Roth, P. Bernier, Chem. Phys. Lett. 387 (2004) 193–197.
[15] R. Droppa Jr., P. Hammer, A.C.M. Carvalho, M.C. dos Santos, F. Alvarez, J. Non-Cryst. Solids 299 (2002) 874.
[16] N. Grobert, W. Hsu, Y. Zhu, J. Hare, H. Kroto, D. Walton, M. Terrones, H. Terrones, P. Redlich, M. Ruhle, Appl. Phys. Lett. 75 (1999) 3363–3365.
[17] M. Yudasaka, R. Kikuchi, Y. Ohki, S. Yoshimura, Carbon 35 (1997) 195–201.
[18] Y. Xing, J. Phys. Chem. B 108 (2004) 19255–19259.
[19] X. Xu, S. Jiang, Z. Hu, S. Liu, ACS Nano 4 (2010) 4292–4298.
[20] C.H. Wang, H.Y. Du, Y.T. Tsai, C.P. Chen, C.J. Huang, L.C. Chen, K.H. Chen, H.C. Shih, J. Power Sources 171 (2007) 55–62.
[21] J.H. Burch, E. Brown, S.A. Contera, N.C. Toledo, D.C. Cox, N. Grobert, L. Hao, J.F. Ryan, J.A. Davies, J. Phys. Chem. C 112 (2008) 1908–1912.
[22] R.L. Jia, C.Y. Wang, S.M. Wang, J. Mater. Sci. 41 (2006) 6881–6888.
[23] W. Li, C. Liang, W. Zhou, Qiu, J.Z. Zhou, G. Sun, Q. Xin, J. Phys. Chem. B 107 (2003) 6292–6299.
[24] M. Freemantle, Chem. Eng. News 74 (1996) 62–66.
[25] Y. Shen, M. Träuble, G. Wittstock, Anal. Chem. 80 (2008) 750–759.
[26] A.J. Bard, L.R. Faulkner, Electrochemical Methods: Fundamentals and Applications , second ed., John Wiley & Sons Inc., 2001.
[27] S. Gottesfeld, I. Raistrick, S. Srinivasan, J. Electrochem. Soc. 134 (1987) 1455–1462.
[28] N. Alexeyeva, E. Shulga, V. Kisand, I. Kink, K. Tammeveski, J. Electroanal. Chem. 648 (2010) 169–175.
[29] U. Paulus, T. Schmidt, H. Gasteiger, R. Behm, J. Electroanal. Chem. 495 (2001) 134–145.
[30] S. Maldonado, K.J. Stevenson, J. Phys. Chem. B 108 (2004) 11375–11383.
[31] S. Maldonado, K.J. Stevenson, J. Phys. Chem. B 109 (2005) 4707–4716.
[32] G. Vijayaraghavan, K.J. Stevenson, Langmuir 23 (2007) 5279–5282.
[33] Q.H. Yang, P.X. Hou, M. Unno, S. Yamauchi, R. Saito, T. Kyotani, Nano Lett. 5 (2005) 2465–2469.
[34] J.W. Jang, C.E. Lee, S.C. Lyu, T.J. Lee, C.J. Lee, Appl. Phys. Lett. 84 (2004) 2877–2879.
[35] D.C. Higgins, D. Meza, Z.W. Chen, J. Phys. Chem. C 114 (2010) 21982–21988.